

Off-diagonal magnetoimpedance in amorphous microwires for low-field magnetic sensors

L. V. Panina^{*,1,2}, N. A. Yudanov¹, A. T. Morchenko¹, V. G. Kostishyn¹, and D. P. Makhnovskiy³

¹ National University of Science and Technology, MISiS, Leninskiy Av. 4, Moscow, Russia

² Institute for Design Problems in Microelectronics RAS, Moscow, Russia

³ School of Marine Science and Engineering, Advanced Composites Manufacturing Centre, Plymouth University, Plymouth PL4 8AA, United Kingdom

Received 31 July 2015, revised 19 November 2015, accepted 20 November 2015

Published online 28 December 2015

Keywords amorphous materials, magnetic anisotropy, magnetic sensors, magnetic wires, magnetoimpedance

* Corresponding author: e-mail lpanina@plymouth.ac.uk, Phone: +79152563580

Magnetoimpedance (MI) in amorphous wires is widely used for the development of various sensors and smart composites with sensing functionalities. In the case of sensor applications, MI in off-diagonal configuration has a number of advantages including linearity, enhanced output voltage sensitivity, efficient resonance, or differential excitation schemes. In this article, we discuss the fundamentals of the off-diagonal MI in amorphous microwires, working principles, and design of miniature MI magnetic sensors. Considering the electrodynamic origin of MI, a comparison with orthogonal fluxgates is

made with the purpose to suggest improvements in MI sensor design. This includes multi-wire configuration and suppression of the voltage offset caused by magnetic anisotropy helicity. New results on the heating effects reveal that the temperature stability along with sensitivity may be enhanced by annealing. The paper focus is aimed to demonstrate that the off-diagonal MI sensors have a high potential for improvements in terms of output voltage sensitivity, magnetic field resolution and temperature stability.

© 2015 WILEY-VCH Verlag GmbH & Co. KGaA, Weinheim

1 Introduction The magnetoimpedance (MI) in soft magnetic conductors demonstrating a very high sensitivity over a wide range of operating frequencies has been recently employed for the development of miniature sensors to detect extremely low magnetic fields, for example, the fields generated by electrical processes of the human heart (MCG [1, 2]). The MI effect includes an enormous change in the high frequency voltage across a magnetic conductor caused by the application of low magnetic fields in the range of few Oersted. In this respect, it can be compared with giant magnetoresistance but high operating frequencies require completely different MI sensor construction. It appears that a simple scheme of measuring the voltage across the MI material involves a number of difficulties associated with nonlinear MI characteristics and relatively low output voltage sensitivity. This scheme, however, is successfully used with thin-film MI materials combined with permanent magnetic layers to shift the operating field point [3–5].

Considering the electrodynamic origin of MI, it can be compared with fluxgates. Usually, fluxgates are divided into two types: parallel and orthogonal, which reflects the mutual directions of the excitation and sensed magnetic fields [6, 7]. They are based on a similar working principle of the periodical magnetization of the core in opposite directions with the driving magnetic field. The sensed field changes the periodicity of the process leading to the generation of even harmonics in the detection signal. The MI is also classified into two categories: diagonal and off-diagonal, which is related to the full surface impedance tensor [8, 9] and the energy consumption in a magnetic conductor under various conditions. The diagonal MI components correspond to the orthogonal direction between the excitation magnetic field and generated electric field, and the off-diagonal components correspond to the parallel direction between these fields. The off-diagonal MI components only occur in magnetic materials characterized by a permeability tensor.

Both fluxgate types can be included in the impedance tensor approach, especially when they operate in the fundamental mode. This paper draws attention on the off-diagonal MI and its advantages for sensor applications, which can be directly compared with the orthogonal fluxgate.

It is interesting to note that the orthogonal fluxgate was proposed with the purpose to simplify the sensor construction as the excitation coil is not needed in this case. The off-diagonal MI needs a detection coil (or excitation coil) so its construction is more complicated than that for the longitudinal diagonal MI when the voltage generated by the passing current is measured across the material. Yet, the off-diagonal configuration for sensing application is preferable because of a number of reasons. Firstly, it may provide a linear vectorial response [10–12]. A high frequency current flowing in materials with a helical static magnetization induces both circumferential and longitudinal ac magnetizations. The time-varying longitudinal magnetization generates a voltage in the coil which is used as the output in off-diagonal MI sensors. The application of an external longitudinal field (sensed field) changes the helical magnetization and the coil voltage. When the sensed field is reversed, the phase of the coil voltage with respect to the excitation current is shifted by π rad so positive and negative fields could be distinguished. Secondly, the off-diagonal MI offers the means to increase the output voltage sensitivity, which is important for improving the noise characteristics [13–15]. Currently, the MI sensor resolution is limited by the electronic noise which is considerably higher than the intrinsic noise of MI materials in a single domain state [16]. Therefore, the MI sensor resolution can be improved by increasing the voltage sensitivity up to a level when the two noise sources are comparable.

The other advantages of the off-diagonal MI sensor scheme based on amorphous glass coated microwires are also considered here, which include the compensation of the offset voltage due to the deviation of the anisotropy from a circumferential direction, optimized excitation methods, multi-wire heads, and temperature stabilization.

A practical off-diagonal MI sensor circuit which is recently commercialized [17] is based on pulse-current excitation. The rise/fall time of the excitation pulses can be made very small with the characteristic frequencies up to GHz. The pulse excitation also includes a dc component which is needed to eliminate the circular domain structure and realize a helical magnetization in the presence of the sensed field. A simple open-loop sensor circuit designed for geomagnetic field detection has a resolution of 160 nT for a dynamic range of ± 1.2 mT [18]. The sensor also has ultra-low power consumption (150 μ A) owing to the pulse excitation. For more sophisticated gradiometer configuration, the equivalent magnetic noise of 1 pT/Hz^{0.5} for frequencies between 20 and 40 Hz was recently achieved without any shielding [19]. The potential of applications in bio-medical field was demonstrated by measuring magnetoencephalogram (MEG) with the field resolution of 50 pT.

In another approach, a harmonic excitation at resonance conditions in combination with an optimized dc bias current

and detection electronics is proposed. The equivalent magnetic noise down to 560 fT/Hz^{0.5} was achieved in the white noise region for frequencies 1–10 kHz [20]. However, for both approaches there is significant $1/f$ noise, but the limiting frequency when this behavior is observed is much higher for harmonic excitation schemes. Yet, the white noise level is still limited by the electronic conditioning, implying that further improvements in sensor design are possible.

2 Principles of off-diagonal MI sensors The off-diagonal MI involves a cross-magnetization process when a high frequency current passing through a ferromagnetic material induces circumferential and longitudinal magnetizations. The occurrence of the longitudinal magnetization requires the existence of the off-diagonal component of the permeability tensor $\mu_{\varphi z}$, where φ, z corresponds to the circumferential and axial directions, respectively. The ac longitudinal magnetization generates a voltage in the coil which is used as the output in off-diagonal MI sensor. A sensitive off-diagonal MI was realized in amorphous wires with circular or helical anisotropy [10, 11, 21, 22], in ribbons with in-plane anisotropy induced by annealing or field quenching [12, 23, 24], and in multilayers with spiral anisotropy [25].

In order to obtain a non-zero $\mu_{\varphi z}$ component, the static magnetization needs to be helical. This is realized in systems with a helical magnetic anisotropy induced, for example, by torque-annealing [22] and is used in inverse Wiedemann effect elements [26, 27]. In the case of a circumferential anisotropy, the application of a dc bias current is needed. In the presence of the axial-sensed magnetic field H_{ex} the magnetization follows a helical pass around it until reaching the saturation. For practical applications, the second method of inducing the helical magnetization is preferable because of a linear response around zero H_{ex} . Although the dc current requires additional power consumption it eliminates the domain structure, thus improving the noise performance.

Typically, the off-diagonal voltage response is understood as a voltage generated in the coil mounted on the MI element (such as a ferromagnetic wire) carrying a high frequency current i_x as shown in Fig. 1a. The coil voltage V_c is defined as

$$V_c = e_\varphi 2\pi a N. \quad (1)$$

Here, e_φ is the circular electric field at the wire surface, a is the wire radius, and N is the number of detection coil turns. The field e_φ is expressed through the wire current i_w using the relationship between the tangential components of electric $\mathbf{e} = (e_z, e_\varphi)$ and magnetic $\mathbf{h} = (h_z, h_\varphi)$ fields at the wire surface: $\mathbf{e} = \hat{\zeta}(\mathbf{h} \times \mathbf{r})$, where $\hat{\zeta}$ is the surface impedance tensor, \mathbf{r} is the unit radial vector directed inside the wire and z -axis is along the wire. Then, Eq. (1) is written as

$$V_c = \frac{4\pi N}{c} \zeta_{\varphi z} i_w. \quad (2)$$

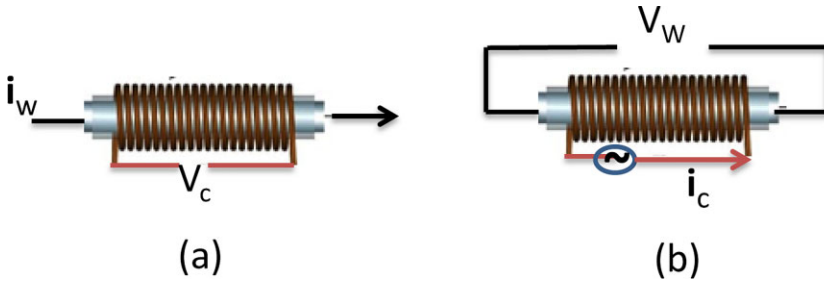


Figure 1 Off-diagonal MI configurations. In (a) the voltage in the coil is generated by the wire current; in (b) the voltage across the wire is generated by the coil current.

In Eq. (2), c is the velocity of light (Gaussian units are used). Therefore, the coil voltage is defined by the off-diagonal component of the surface impedance tensor. The other off-diagonal configuration utilizes the wire voltage induced by the coil current as shown in Fig. 1b.

$$V_w = e_z l = -\zeta_{z\varphi} h_z l = -\frac{4\pi N_1}{c} \zeta_{z\varphi} i_c, \quad (3)$$

N_1 is the number of turns in the excitation coil. The voltage responses defined by Eqs. (2) and (3) are referred to as off-diagonal MI as they are proportional to the off-diagonal components of the surface impedance tensor $\zeta_{z\varphi} = \zeta_{\varphi z}$. At high frequencies and low excitation fields the ac permeability tensor is defined by a small precession of the magnetization around its static direction resulting in non-zero $\mu_{\varphi z}$. A similar working principle is realized in the orthogonal fluxgates operating in a fundamental mode when the magnetization oscillates around saturation without changing polarity.

Equations (2) and (3) describe pure off-diagonal excitation/detection schemes. They can be also used together with the diagonal schemes of inducing the wire voltage by the passing current or the coil voltage by the coil current. In general, we can introduce the impedance matrix [11] which relates the voltage vector V and the current vector i according to

$$V = \hat{Z}i, \quad V = \begin{pmatrix} V_w \\ V_c \end{pmatrix}, \quad i = \begin{pmatrix} i_w \\ i_c \end{pmatrix}, \quad (4)$$

$$\hat{Z} = \begin{pmatrix} \frac{2l}{ca} \zeta_{zz} & -\frac{4\pi N_1}{c} \zeta_{z\varphi} \\ \frac{4\pi N}{c} \zeta_{\varphi z} & \frac{8\pi^2 N N_1}{c} \zeta_{\varphi\varphi} \end{pmatrix}.$$

In Eq. (4), ζ_{zz} and $\zeta_{\varphi\varphi}$ are diagonal components of the surface impedance tensor. This generalized approach based on the impedance tensor is useful to describe various excitation/detection schemes. The diagonal component Z_{zz} determines a usual MI voltage, $Z_{\varphi\varphi}$ corresponds to a parallel fluxgate. Equation (4) also contains a mixed excitation, for example, the wire voltage can be induced by the combination of i_w, i_c . This could be of interest for producing asymmetric voltage response without use of a dc bias [28, 29].

A detailed analysis of the surface impedance $\hat{\zeta}$ valid at arbitrary frequencies can be found in [8, 9]. Here we will give the high frequency approximation for the impedance tensor of a single domain wire when the skin-effect is strong

$$\hat{\zeta} = (1-j) \sqrt{\frac{\omega}{8\pi\sigma}} \begin{pmatrix} \sqrt{\mu_{\text{ef}} \cos^2 \theta + \sin^2 \theta} & (\sqrt{\mu_{\text{ef}}} - 1) \cos \theta \sin \theta \\ (\sqrt{\mu_{\text{ef}}} - 1) \cos \theta \sin \theta & \sqrt{\mu_{\text{ef}} \sin^2 \theta + \cos^2 \theta} \end{pmatrix}. \quad (5)$$

In Eq. (5), j is the imaginary unit, ω is the angular frequency of the electromagnetic field, μ_{ef} is the permeability parameter composed of the components of the rotational permeability tensor, and θ is the angle between the static magnetization and the wire axis. Equation (5) demonstrates that the magnetic field dependence of $\hat{\zeta}$ is related to the field behavior of the dynamic permeability μ_{ef} and static magnetization angle θ . In the case of a circumferential anisotropy, the external field H_{ex} applied along the wire rotates the magnetization toward the axis and to a great extent this process determines the sensitivity of $\hat{\zeta}$ in the field region $|H_{\text{ex}}| < H_K$, where H_K is the effective anisotropy field. It is also clear that the diagonal components do not depend on the magnetization polarity, whereas the off-diagonal components change the sign if the magnetization is reversed (say, by H_{ex}). In the case of a circumferential anisotropy, $\zeta_{z\varphi} (\zeta_{\varphi z})$ dependence on H_{ex} is almost linear in the field range $|H_{\text{ex}}| < H_K/2$. Therefore, the off-diagonal impedance can be used in a linear vectorial sensor. If the wire has an ideal circular domain structure, the off-diagonal surface impedance in the domains with opposite polarities in the circular direction has opposite signs, therefore, the averaged off-diagonal response over domains is null. The circular domain structure should be removed by applying a dc bias current producing a circular bias field H_b .

In practice, the anisotropy has some deviations from the circular direction which can give rise to an output voltage for a zero H_{ex} . Figure 2 shows the theoretical off-diagonal impedance plots Z_{off} versus H_{ex} for wires with a slightly helical anisotropy and different bias fields. The real and imaginary parts of Z_{off} go through zero and change signs at some negative value of H_{ex} having almost linear behavior near this field. With increasing the bias field the sensitivity drops. The offset impedance can be compensated by using positive and negative dc bias currents. This is illustrated in Fig. 3. When $H_{\text{ex}} = 0$, the magnetization has angles θ and

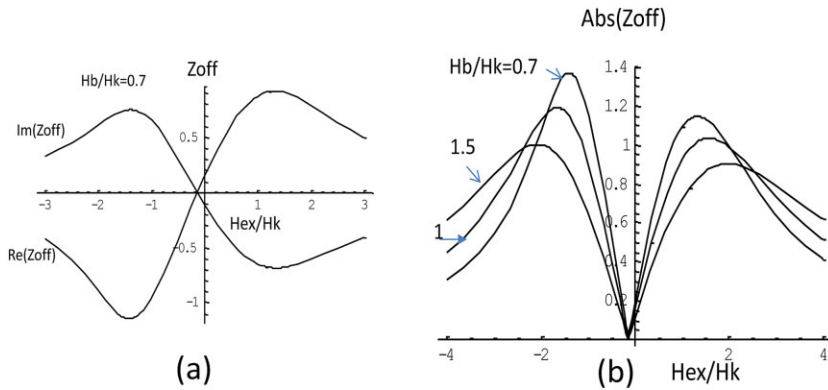


Figure 2 Field plots of the off-diagonal magnetoimpedance in single-domain wires with a helical anisotropy having an angle of 82° with respect to the wire axis at a frequency of 10 MHz. In (a) real and imaginary parts for a bias field $H_b/H_K = 0.7$. In (b) the magnitude for different bias fields ($H_b/H_K = 0.7, 1, 1.5$). The impedance is normalized on the maximum value of the real part at $H_b/H_K = 0.7$. The other parameters are: saturation magnetization – 500 G, anisotropy field $H_K = 2.5$ Oe, conductivity $100 \mu\Omega$, the wire radius $a = 10 \mu\text{m}$.

$\theta_1 = -\pi + \theta$ with respect to the z -axis, for positive and negative dc bias, respectively, so $\cos \theta \sin \theta$ does not change. In the presence of H_{ex} , the characteristics are reversed (with respect to the offset level). Therefore, subtracting the off-diagonal voltages for positive and negative bias the offset will be canceled. A practical technique to suppress the offset due to anisotropy helicity was proposed for orthogonal fluxgates [30]. The bias was inverted periodically at a frequency much lower than the excitation frequency. To avoid the effect of bias reversing on the noise, the periods before and after the transition could be excluded either digitally [31] or analogously [32] using a fast solid state switch.

3 Experimental methods for off-diagonal MI

A most appropriate way to measure the surface impedance at high frequencies is with the help of two-port Vector Network Analyzer configured for S-parameter measurements [33, 34]. For example, forward transmission $S_{21} = V_{in}/V_{out}$ can be used where V_{in} is the excitation sinusoidal signal from Port 1 and V_{out} is the output signal measured in Port 2. In the case of the off-diagonal component, the ac excitation current i_w is set by V_{in} , whereas V_{out} is equal to V_c , so the S_{21} -parameter is directly proportional to Z_{off} or $\zeta_{\varphi z}$. Note that S_{21} -parameter includes both the normalized amplitude $|V_{in}/V_{out}|$ and phase shift $\text{Arg}(V_{in}/V_{out})$ with respect to the excitation signal. Within this method, the excitation signal can be made very small producing a wire current in the range of mA to exclude nonlinear magnetization dynamics. Larger excitation

currents may be used in practical sensor design for generation of the second harmonic signal [35].

The measured sample is placed onto an open-type cell as shown in Fig. 4 made of copper-coated fiberglass printed circuit board (PCB). The connection stripes have a geometry providing the wave impedance in the order of 50Ω over a wide frequency range. A wire element (of about 10 mm long) soldered or bonded to the cell is excited by the sinusoidal input voltage V_{in} . The output voltage V_{out} is taken from a tiny coil. The S_{21} -parameter is measured as a function of the external magnetic field H_{ex} applied along the wire with the help of a solenoid or a Helmholtz coils.

The complex-valued $S_{21}(H_{ex})$ as a measure of the off-diagonal impedance is shown in Fig. 5 at a fixed frequency of 100 MHz for different bias currents using a CoFeSiB amorphous wire with well-defined circumferential anisotropy. The signal is very small if no dc bias is applied and increases sharply with increasing I_b . Typically, the coercivity in amorphous wires with nearly zero magnetostriction is about a fraction of Oe and applying a small current of few mA (2.5 mA in Fig. 5) should magnetize the wire in the circular direction. With increasing I_b the magnetic hardness in the circular direction also increases

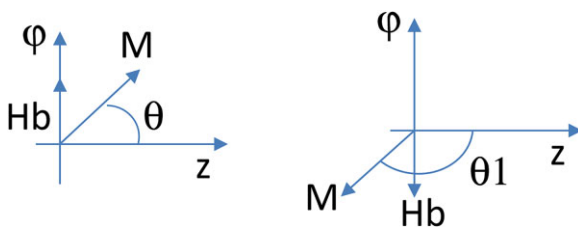


Figure 3 Illustration of the method of canceling the offset voltage.

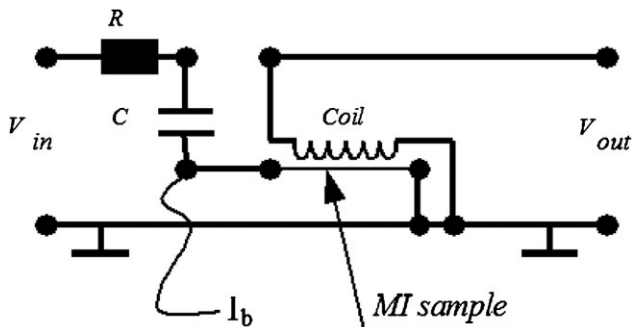


Figure 4 Electric circuit of the cell for the off-diagonal impedance measurement. Blocking capacitor (C) is needed to cut the dc current flow to the analyzer ports. Terminal resistors are required for normalizing input/output impedance of the measured elements.

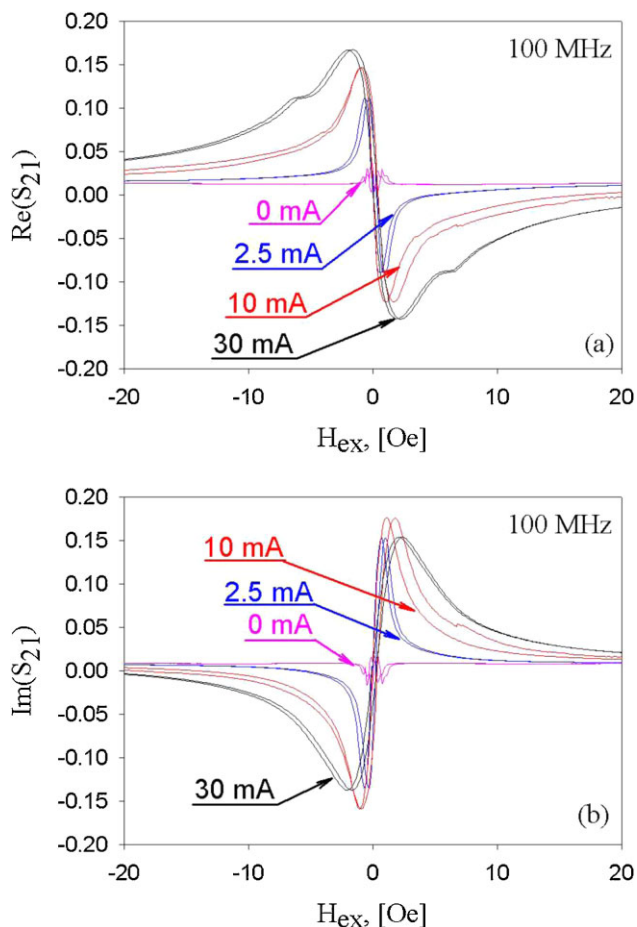


Figure 5 Off diagonal impedance represented by S_{21} -parameter for different dc bias currents for a wire of $\text{Co}_{66.94}\text{Fe}_{3.83}\text{Ni}_{1.44}\text{B}_{12.29}\text{Si}_{15.56}$ composition with a total diameter of $22\ \mu\text{m}$ and the metal core diameter of $19.6\ \mu\text{m}$.

and the sensitivity of the off-diagonal response is expected to drop. However, in the low field region the sensitivity almost does not change with increasing I_b , but the maximum of S_{21} continuously to increase. This trend is not seen in the theoretical plots of Fig. 2 obtained for a single domain state and suggests that the surface regions of the wire may need stronger dc bias to provide a uniform circular magnetization. The real and imaginary parts of the off-diagonal component change sign when H_{ex} is reversed having almost a linear region between the two peaks. The field interval of the linear behavior increases with increasing I_b and constitutes about $\pm 2\ \text{Oe}$ for $I_b = 30\ \text{mA}$.

A pulse current excitation of the wire supplied by CMOS IC multivibrator or a microcontroller is often used in off-diagonal MI sensors [36–38], which provides both high frequency and dc currents to the wire. Figure 6 shows the output signals when the wire is excited by a square pulse train with a small rise (fall) times. In the presence of the external field, the output signal has two sharp pulses of different polarity which changes if the field is reversed. In this case, the output is characterized by the pulse amplitude

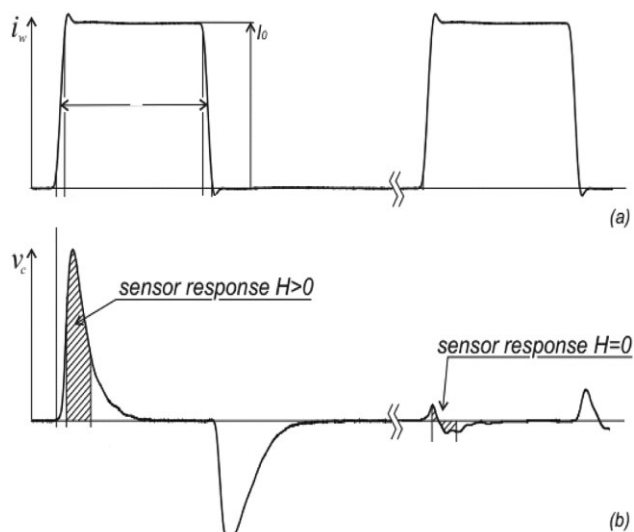


Figure 6 Pulse excitation signal (a) and off-diagonal output (b). The time of pulse rise (drop) is about 20 ns, which corresponds to a characteristic frequency of 50 MHz.

and polarity also allowing the vectorial measurement (amplitude and sign) of the external magnetic field.

This output is rectified by a circuit containing a digital switch and an integrating chain to obtain a smooth quasi-dc signal which is proportional to the pulse amplitude and multiplied by the polarity as shown in Fig. 7.

The off-diagonal sensor sensitivity can be increased by increasing the number of the detection coil turns and the excitation frequency. However, the detection circuit has a parasitic capacitance and represents RLC circuit with intrinsic resonance frequency. The excitation at the resonance frequency results in the maximum of the output voltage and voltage sensitivity. Therefore, the number of turns and the excitation frequency should be balanced with respect to the resonance conditions and the intrinsic impedance sensitivity. In this respect, a harmonic excitation with a dc bias current can have advantages as all the

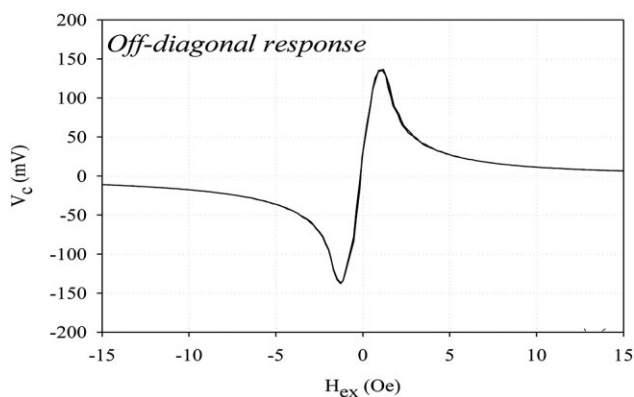


Figure 7 Rectified and amplified output obtained after pulse excitation of amorphous microwire having off-diagonal characteristics shown in Fig. 5.

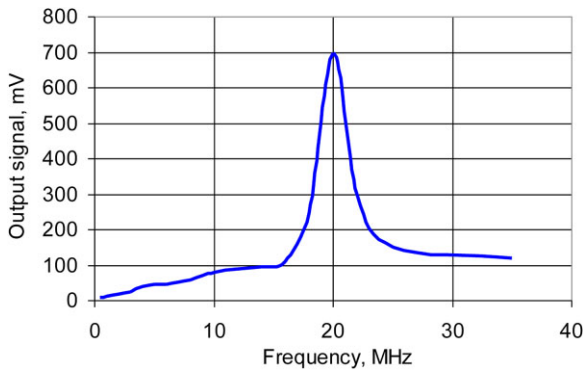


Figure 8 Frequency characteristic of the output signal from the coil when the wire is excited by a sinusoidal current. The wire being 8 mm long had a composition of $\text{Co}_{66.94}\text{Fe}_{3.83}\text{Ni}_{1.44}\text{B}_{11.57}\text{Si}_{14.59}\text{Mo}_{1.69}$, the metal core diameter was $40\ \mu\text{m}$, the total diameter was $46\ \mu\text{m}$. The detection coil had 55 turns of $40\ \mu\text{m}$ diameter Cu wire mounted directly on the wire. The axial magnetic field was 1 Oe and a dc bias current was 7.7 mA.

parameters influencing the voltage sensitivity can be easier adjusted. Figure 8 shows the output voltage amplitude versus excitation frequency for the off-diagonal MI wire element, which demonstrates a sharp peak occurring at the LC-resonance frequency of the detection circuit. The optimization of the operational frequencies in the orthogonal fluxgates was also considered to improve the sensitivity and signal-to-noise ratio [39].

There is one more off-diagonal configuration as described by Eq. (3), when the magnetic wire is excited by a high-frequency magnetic field produced by the coil mounted on the wire and the voltage signal is measured across the wire. This off-diagonal configuration may not be preferable as the coil self-inductance limits the generated magnetic field at high frequencies.

4 Multi-wire configuration of the off-diagonal MI

Recently, there is an attempt to tailor the MI response by utilizing a number of magnetic wires by means of their magneto dipole interaction [40–42]. In the case of off-diagonal MI, the configuration is similar to the multicore orthogonal fluxgate having n -wires connected in parallel [43–45]. Each wire is excited by a current of the same amplitude and frequency. Originally, this was proposed in order to enlarge the cross-sectional area and to increase proportionally the output voltage. However, in orthogonal fluxgates it was found that the sensitivity may increase exponentially when $n > 4$: a sensitivity of 16-wire core is 65 times higher than the sensitivity of a single wire. Such enhancement occurs when the wires are packed close together so it was assumed that the magnetic dipole interaction was responsible for this. Later, it was proven that the main cause of the anomalous sensitivity increase is the improvement of the quality factor of the tuning circuit [46]. The noise is also lower for multicore configuration with closely spaced wires.

We propose a multi-wire approach in attempt to improve the output voltage sensitivity of the off-diagonal MI and to increase the dynamic range. For miniature sensors and high frequency excitation, the use of a large number of wires is not of interest so the off-diagonal response of two- and three-wire core was investigated. The dc hysteresis loops for a single wire and two closely spaced wires (glass-coated wires were used so the separation between the wires equals the glass coating) are shown in Fig. 9. The loops are almost linear with the saturation at the anisotropy field which is typical of a circumferential anisotropy. The magnetization slope is decreased for a wire-pair in comparison with that for a single wire and the effective anisotropy field increases to $120\ \text{A m}^{-1}$ from $75\ \text{A m}^{-1}$ for a single wire. This clearly demonstrates the effect of the magnetostatic interaction between the wires due to the stray fields which is more pronounced at higher fields when the longitudinal magnetization is increased.

The off-diagonal MI response of a wire-pair was compared with that of a single wire. The sensor head with two wires is shown in Fig. 10. The head is excited by the same total current $i_w + I_b$ as in the case of a single wire (so in the wire-pair head each wire carries a current $(i_w + I_b)/2$). In Fig. 11, the responses from single- and two-wire heads are given. The voltage peak of a single-wire head seen in Fig. 11 is lower in comparison with that given in Fig. 8. In this experiment, the wire of different alloy composition and diameter was used, so the excitation frequency was not optimal. It is seen that the sensitivity is a little lower for the wire-pair because of the stray field influence (the sensitivity increase due to larger amount of magnetic material is excluded when using the same i_w). There is an increase in the full scale range and maximum of the output voltage. This behavior is similar to the effect of bias current increase (compare with Fig. 5) or using the detection coil for feedback [15]. When three wires are used with similar excitation conditions, the sensitivity drops noticeably due to

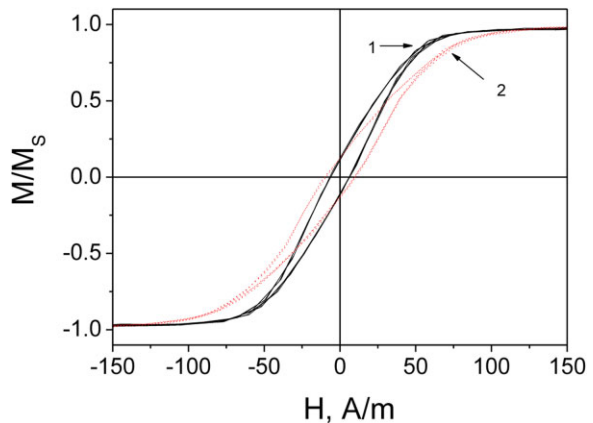


Figure 9 Hysteresis loops of single (1, black curve) and two (2, red curve) glass-coated $\text{Co}_{67}\text{Fe}_{3.9}\text{Ni}_{1.5}\text{B}_{11.5}\text{Si}_{14.5}\text{Mo}_{0.6}$ microwires. The metal core diameter was $29.2\ \mu\text{m}$, the total diameter was $31\ \mu\text{m}$.

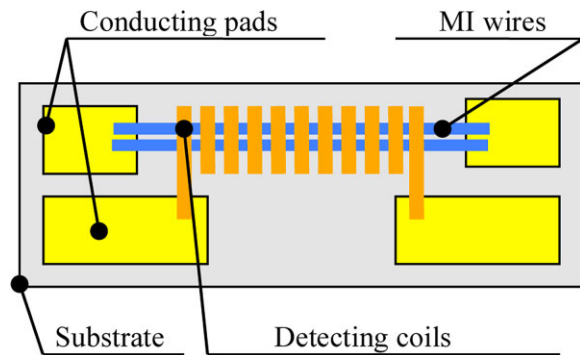


Figure 10 Schematics of two-wire off-diagonal sensor head. The wires are electrically connected in parallel at their ends and the detection coil is mounted directly on the wires.

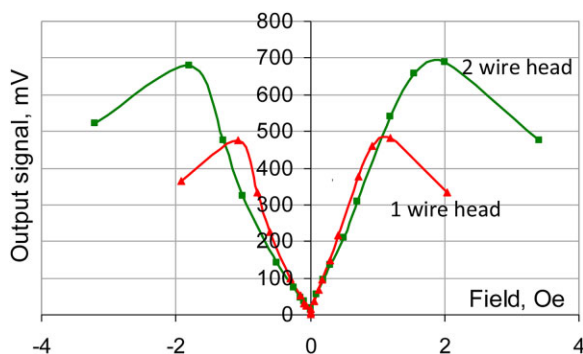


Figure 11 Output signal amplitude versus magnetic field of the off-diagonal MI heads with single wire and two-wire cores. The excitation voltage included a dc component which generated a total dc current of 7.7 mA. The excitation frequency was 20 MHz. The wire parameters are the same as for Fig. 9.

stronger interaction between the wires. However, the sensitivity could be tuned by changing the dc bias in each wire. So the multi-wire MI head could be advantageous to increase the voltage sensitivity and dynamic range. The noise characteristics are expected to be improved as the random noise is proportional to \sqrt{n} .

5 Temperature effects on the off-diagonal MI response with glass-coated wires In amorphous microwires the magnetic structure and MI effect may show considerable temperature variations in the working range of -20 to 80 °C, although these temperatures are well below the Curie temperature [47, 48]. Up to present, there are very limited investigations of the temperature dependence of MI in glass-coated microwires. This section discusses the variations of the off-diagonal impedance with temperature cycles and the methods of temperature stability improvement, which is crucial for commercial use of MI sensors.

The MI sensitivity strongly depends on the effective anisotropy, which is of a magnetoelastic origin in amorphous wires. The internal stress occurs in the process

of rapid solidification and is quite different in wires with different ratios of the metal core to the glass thickness [49]. This can be caused by the difference in thermal expansion coefficients of glass and metal. When a microwire is heated the residual stress is partially released changing the effective anisotropy. In a recent work [48], it was demonstrated that heating to a moderate temperatures 60 – 100 °C changes the angle of a surface helical anisotropy in near-zero magnetostrictive wires. Altering the anisotropy inevitably will lead to the temperature dependence of MI.

Figure 12 shows the plots of the off-diagonal MI response and the average sensitivity for different temperatures: during heating the sensitivity increases with temperature until 60 °C and starts to fall as the temperature if further increased. The drop in the sensitivity, output peak value, and peak magnetic field at higher temperatures should

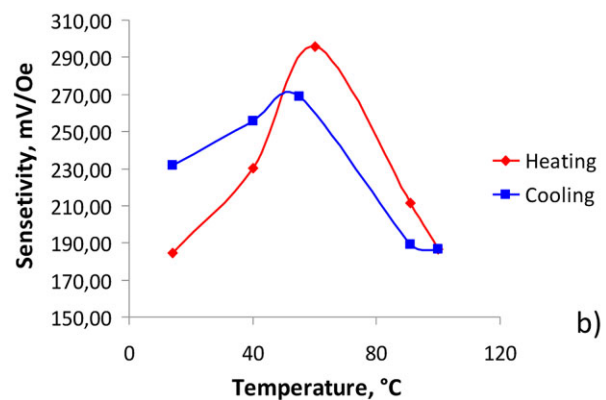
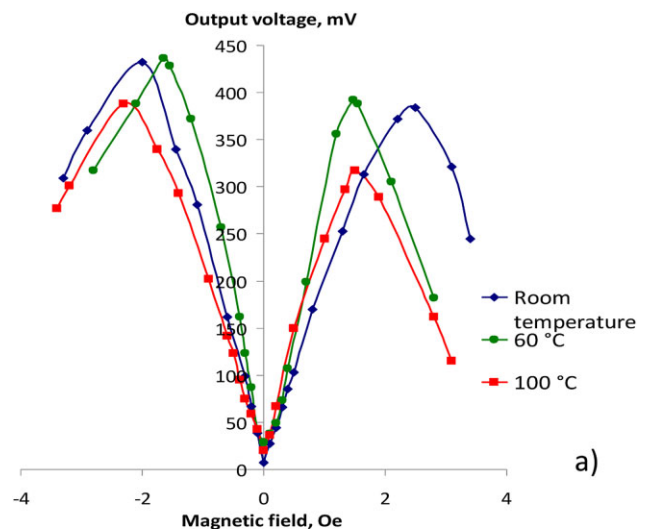


Figure 12 In (a) output voltage versus magnetic field of the off-diagonal MI sensor for different temperatures during heating and in (b) average sensitivity defined in the field range 1.5 Oe during heating–cooling cycle. The wire of composition $\text{Co}_{67}\text{Fe}_{4.1}\text{Ni}_{1.46}\text{B}_{11.6}\text{Si}_{14.6}\text{Mo}_{1.69}$ with metal core diameter of 36 μm and total diameter of 42 μm was used. The excitation frequency was 20 MHz and the dc bias current was 14.4 mA.

be related with larger anisotropy distribution due to non-uniform stress relaxation at the glass-metal interface. There are also large variations with temperature in the sensor output at higher fields. Upon cooling down to room temperature, the MI characteristics are not repeatable, revealing irreversible change in the internal stress distribution. The MI sensitivity as a function of temperature along the heating-cooling cycle is shown in Fig. 12b. It is seen that after heating, the temperature dependence of MI becomes weaker. This behavior suggests that proper heat treatments may improve the temperature stability of MI.

It is known that various annealing regimes may considerably change the magnetic structure of glass-coated wires [50, 51]. Joule annealing typically improves the magnetic softness and increases the MI sensitivity. Annealing by heating can be easily applied to the entire MI sensing head without changing its circuitry, so this technique is attractive for device applications. We have demonstrated that annealing of the whole off-diagonal MI sensor head integrated into the detection circuit helps to improve both the sensitivity and temperature stability. The annealing regime should be chosen depending on the wire composition and geometry. Figure 13 shows the plots of the coil voltage amplitude versus magnetic field before and after annealing at different temperatures during a short time of 2–3 min. Annealing at moderate temperatures increases the MI sensitivity due to a partial stress release. However, higher annealing temperatures (higher than 160 °C for Co-rich amorphous wires with relatively thin glass coating) result in substantial drop in sensitivity. This can be related with irregularities of the internal stress distribution due to the relaxation processes of amorphous structure at higher

temperatures, which leads to greater anisotropy distribution and broader MI characteristics.

After annealing, the whole off-diagonal MI sensing head, the temperature stability is improved. Optimal annealing stabilizes the sensor output in a certain magnetic field range, where the sensitivity changes less than few percent. Thus, the sensitivity of MI sensor head with the characteristics shown in Fig. 13, changes within 2–3% for temperatures up to 90 °C in the field range of ± 0.7 Oe. For higher fields, the temperature effect is greater: the maximum of the voltage amplitude decreases with temperature by about 10%. Nevertheless, we demonstrated the efficiency of the heat treatments to improve the temperature stability. The detailed investigation of the temperature effects on MI will be published elsewhere.

6 Conclusions This article discusses the off-diagonal magnetoimpedance (MI) in amorphous microwires including the physical mechanisms, methods of measurements, and operational principles of high-sensitivity magnetic field sensors utilizing this effect. A comparison with orthogonal fluxgates operating at fundamental mode is made demonstrating similarities and differences. This comparison also suggests some improvements in off-diagonal MI sensor design, such as multiwire configuration, suppression of the voltage offset due to anisotropy helicity, resonance detection circuits. We also discuss new results on temperature effect on MI and annealing as methods to improve both the sensitivity and temperature stability. The main conclusion of the presented analysis is that the off-diagonal MI sensors which already have a pT resolution in the white noise region have a high potential for improvements in terms of sensitivity, temperature stability, and spatial resolution.

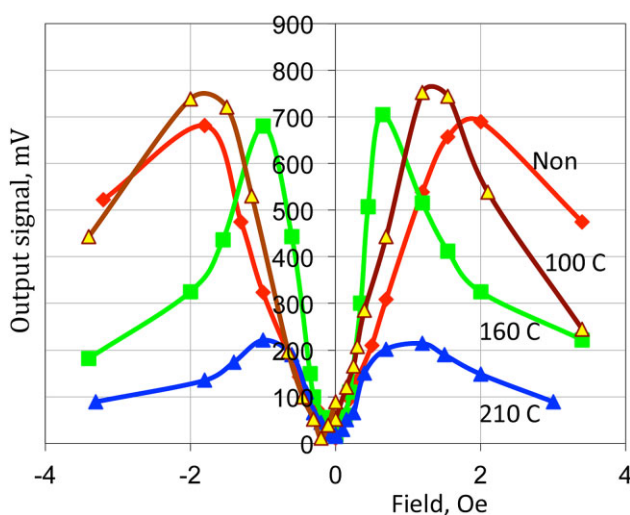


Figure 13 Output voltage of the off-diagonal MI after annealing the sensor head at different temperatures during 2–3 min. The wire of composition $\text{Co}_{66.94}\text{Fe}_{3.83}\text{Ni}_{1.44}\text{B}_{11.57}\text{Si}_{14.59}\text{Mo}_{1.69}$ with metal core diameter of 40 μm and total diameter of 46 μm is used. The excitation frequency was 20 MHz and the dc bias current was 14.4 mA.

Acknowledgements This work was supported by the Russian Federation State contract for organizing a scientific work and partially supported by the Russian Foundation for Basic Research, grant no. 13-08-01319 and NUST MISIS grant NoK3-2015-060. The authors are very thankful to Dr. V. S. Larin, MFTI Ltd., for donating the wire samples.

References

- [1] K. Mohri, Y. Honkura, L. V. Panina, and T. Uchiyama, *J. Nanosci. Nanotechnol.* **12**, 7491 (2012).
- [2] T. Uchiyama, S. Nakayama, K. Mohri, and K. Bushida, *Phys. Status Solidi A* **206**, 639 (2009).
- [3] S. N. Nejad, A. A. Fomani, and R. R. Mansour, *Conference Publication, Sensors 2013 IEEE*, art. no. 6688221.
- [4] Y. Nishibe and N. Ohta, *R&D Rev. Toyota CRDL* **35**, 1 (2000).
- [5] A. Takayama, T. Umehara, A. Yuguchi, and H. Kato, *IEEE Trans. Magn.* **35**, 3643 (2002).
- [6] P. Ripka, *Sens. Actuators A* **106**, 8 (2003).
- [7] S. H. Choi, *IEEE Trans. Magn.* **47**, 2573 (2011).
- [8] D. P. Makhnovskiy, L. V. Panina, and D. J. Mapps, *Phys. Rev. B* **63**, 144424 (2001).
- [9] M. Knobel and K. R. Pirota, *J. Magn. Magn. Mater.* **242–245**, 33 (2002).

- [10] A. S. Antonov, I. T. Iakubov, and A. N. Lagarkov, *IEEE Trans. Magn.* **33**, 3367 (1997).
- [11] S. Sandacci, D. Makhnovskiy, L. Panina, K. Mohri, and Y. Honkura, *IEEE Trans. Magn.* **40**, 3905 (2004).
- [12] M. Malateka and L. Kraus, *Sens. Actuators A* **164**, 41 (2010).
- [13] B. Dufay, S. Saez, C. Dolabdjian, A. Yelon, and D. Menard, *IEEE Sens. J.* **11**, 1317 (2011).
- [14] C. Dolabdjian, A. Yelon, and D. Menard, *IEEE Sens. J.* **13**, 379 (2013).
- [15] B. Dufay, S. Saez, C. Dolabdjian, A. Yelon, and D. Menard, *IEEE Trans. Magn.* **49**, 85 (2013).
- [16] L. G. C. Melo, D. Menard, A. Yelon, L. Ding, S. Saez, and C. Dolabdjian, *J. Appl. Phys.* **103**, 033903 (2008).
- [17] Y. Honkura, *J. Magn. Magn. Mater.* **249**, 375 (2002).
- [18] C. M. Cai, T. Nagao, M. Mori, and M. Yamamoto, in: *Proc. All Toyota Research Workshop*, April 2010.
- [19] T. Uchiyama, K. Mohri, Y. Honkura, and L. V. Panina, *IEEE Trans. Magn.* **48**, 3833 (2012).
- [20] M. Malatek, B. Dufay, S. Saez, and C. Dolabdjian, *Sens. Actuators A* **204**, 20 (2013).
- [21] M. Ipatov, V. Zhukova, J. M. Blanco, J. Gonzales, and A. Zhukov, *Phys. Status Solidi A* **205**, 1779 (2008).
- [22] M. L. Sánchez, M. V. Prida, J. D. Santos, J. Olivera, T. Sánchez, J. García, M. J. Pérez, and B. Hernando, *Appl. Phys. A* **104**, 433 (2011).
- [23] T. Sánchez, V. Vega, J. D. Santos, M. J. Pérez, V. M. Prida, M. L. Sánchez, Ll., Escoda, J. J. Suñol, and B. Hernando, *Phys. Status Solidi A* **208**, 2265 (2011).
- [24] N. A. Buznikov, C. G. Kim, C. O. Kim, and S. S. Yoon, *J. Magn. Magn. Mater.* **309**, 216 (2007).
- [25] N. Fry, D. P. Makhnovskiy, L. V. Panina, S. I. Sandacci, D. J. Mapps, and M. Akhter, *IEEE Trans. Magn.* **40**, 3358 (2004).
- [26] L. Kraus, M. Malatek, and M. Dvorak, *Sens. Actuators A* **142**, 468 (2008).
- [27] P. Bobes-Limenes, J. A. Garcia, J. Carrizo, M. Rivas, and J. C. Martinez-Garcia, *Sens. Actuators A* **180**, 45 (2012).
- [28] L. V. Panina, *J. Magn. Magn. Mater.* **249**, 278 (2002).
- [29] L. V. Panina, D. P. Makhnovskiy, and D. J. Mapps, *Appl. Phys. Lett.* **77**, 121 (2000).
- [30] I. Sasada, *IEEE Trans. Magn.* **38**, 3377 (2002).
- [31] E. Weiss, E. Paperno and A. Plotkin, *J. Appl. Phys.* **107**, 09E717 (2010).
- [32] J. Kubik, P. L. Ripka, and P. Kaspar, *IEEE Sensors J.* **7**, 179 (2007).
- [33] D. P. Makhnovskiy, L. V. Panina, and D. J. Mapps, *J. Appl. Phys.* **87**, 4804 (2000).
- [34] D. P. Makhnovskiy, L. V. Panina, and D. J. Mapps, *J. Appl. Phys.* **89**, 7224 (2001).
- [35] L. Kraus, *IEEE Trans. Magn.* **46**, 428 (2010).
- [36] K. Mohri, T. Uchiyama, L. P. Shen, C. M. Cai, and L. V. Panina, *Sens. Actuators A* **91**, 85 (2001).
- [37] N. Kawajiri, M. Nakabayashi, C. M. Cai, K. Mohri, and T. Uchiyama, *IEEE Trans. Magn.* **35**, 3667 (1999).
- [38] B. Fisher, L. V. Panina, D. J. Mapps, and N. Fry, *IEEE Trans. Magn.* **49**, 89 (2013).
- [39] Y.-H. Kim, Y. Kim, C.-S. Yang, and K.-H. Shin, *J. Magnetism* **18**, 159 (2013).
- [40] J. Devkota, A. Ruiz, P. Mukherjee, H. Srikanth, M. H. Phan, A. Zhukov, and V. S. Larin, *J. Alloys Compd.* **549**, 295 (2013).
- [41] C. Garcia, V. Zhukova, A. Zhukov, N. Usov, M. Ipatov, J. Gonzalez, and J. M. Blanco, *Sens. Lett.* **5**, 1 (2007).
- [42] H. Chiriac, D. D. Herea, and S. Corodeanu, *J. Magn. Magn. Mater.* **311**, 425 (2007).
- [43] X. P. Li, J. Fan, J. Ding, H. Chiriac, and X. B. Qian, *J. Appl. Phys.* **99**, 08B313 (2006).
- [44] F. Jie, N. Ning, W. Ji, H. Chiriac, and X. P. Li, *IEEE Trans. Magn.* **45**, 4451 (2009).
- [45] P. Ripka, X. P. Li, and F. Jie, *Sens. Actuators A* **156**, 265 (2009).
- [46] P. Ripka, M. Butta, F. Jie, and X. P. Li, *IEEE Trans. Magn.* **46**, 654 (2010).
- [47] M. Kurniawan, R. K. Roy, A. K. Panda, D. W. Greve, P. R. Ohodnicki, and M. E. McHenry, *J. Appl. Phys.* **105**, 222407 (2014).
- [48] A. Chizhik, A. Maziewski, A. Zhukov, and J. Gonzalez, *J. Magn. Magn. Mater.* **400**, 356 (2016).
- [49] V. Zhukova, A. Chizhik, A. Zhukov, A. Torcunov, V. Larin, and J. Gonzalez, *IEEE Trans. Magn.* **38**, 3090 (2002).
- [50] A. Talaat, V. Zhukova, M. Ipatov, J. M. Blanco, L. Gonzalez-Legarreta, B. Hernando, J. Gonzalez, and A. Zhukov, *J. Appl. Phys.* **115**, 17A313 (2014).
- [51] A. Zhukov, A. Talaat, J. M. Blanco, M. Ipatov, and V. Zhukova, *J. Electron. Mater.* **43**, 4532 (2014).